MATHEMATICAL MODELLING AND EXPERIMENTAL STUDY OF ELECTRODYNAMIC CONTROL OF SWIRLING FLAME FLOWS

Harijs Kalis[1], Inesa Barmina[1], Maija Zake[1], Andrejs Koliskins[2]
[1]University of Latvia, [2]Riga Technical University, Latvia
kalis@lanet.lv, mzfi@sal.lv, akoliskins@rbs.lv

Abstract. Mathematical modelling and experimental study of the electric field control of combustion dynamics and development of exothermal combustion of volatiles downstream the swirling flame flow at biomass thermo chemical conversion are carried out with the aim to provide electric control of the combustion characteristics and to improve combustion conditions in the flame reaction zone. A mathematical model is developed for fuel combustion in a cylindrical pipe for an inviscid, compressible, axially symmetric swirling flow, which considers the development of the exothermic reaction of fuel combustion and approximation of the reaction rate by first-order Arrhenius kinetics. The goal of the mathematical modelling is to illustrate the development of the flow velocity, temperature and composition fields and stream function provided the electric field is applied to the flame and considering its effects on development of the swirling flame reaction zone. The approximations of non-linear problems and development of fuel combustion are based on implicit finite-difference and alternating direction (ADI) methods.

Keywords: swirling flame, biomass, combustion of volatiles, electric field.

Introduction

Because still growing interest to the utilization of biomass residues (wood, straw, etc.) for cleaner and more effective heat energy production different biomass combustion systems are being developed. To provide an enhanced biomass thermo chemical conversion with improved combustion characteristics, different technical solutions for combustion control can be used [1-4], which include the swirl-enhanced mixing of the flame components along with the stabilization of the flame reaction zone [1], the co-combustion and co-firing of biomass with a fossil fuel [2], as well the electric [3] and magnetic field [4] control of combustion dynamics. Previous experimental studies of the electric field effects on the flame formation and combustion characteristics have shown [5; 6] that the application of the electric field to the swirling flame flow can result in significant changes in the flame shape, size and combustion characteristics due to the development of processes which can be related to the electric field-induced heat and mass transport of flame species in the field direction which initiates local variations of the flame temperature, combustion efficiency and composition of the products. In addition to the electric field-enhanced mass transport of the flame species, the development of combustion dynamics downstream the swirling flame flow can be affected by a magnetic field-induced Lorentz force at the bottom of the combustor. With the above said, the main aim of the recent study was to perform complex mathematical modelling and experimental study of the electric field-induced variations of the combustion dynamics at thermo chemical conversion of biomass (wood) pellets along with the estimation of the effects which can be related to the electric field-induced magnetic force affecting the development of the swirling flame temperature and velocity field with local variations of the stream function. A mathematical model has been developed for simple chemical reaction, which considers the field-induced formation of the axial and radial components of the electric current at the bottom of the flame reaction zone, with the swirling flame flow and field-induced development of the fuel combustion downstream the cylindrical combustor of the radius r_0. The results of the numerical simulation show that increasing the field-induced current at the bottom of the combustor, which determines the growth of the electrodynamic force parameter P_e, results in a field-enhanced variation of the stream function that increases the maximum flow velocity, flow vorticity, peak flame temperature and the chemical reaction rate. The results of the mathematical modelling are compared with the results of the experimental study of the combustion processes developing at thermo chemical conversion of biomass pellets downstream the swirling flame flow, if an axial symmetric electric field is applied to the swirling base determining the electric current generation, which leads to the field-induced local variations of the flow velocity, swirl intensity, flame temperature, composition and combustion efficiency.

Experimental device

The electric field effect on the processes of biomass (wood pellets) thermo chemical conversion is studied experimentally using a batch-size pilot device with a heat output up to 2 kW. The pilot device combines a biomass gasifier with primary air supply at the bottom of the combustor, which produces the axial flow of volatiles, and swirling secondary air supply at the bottom of the combustor determining the development of the swirling combustion of volatiles (Fig. 1-a). The biomass gasifier is filled with 240 g wood pellets (6 mm in diameter and from 5m to 15 mm in length). Elemental composition of wood pellets is characterized by: 50.2 % of carbon content; 5.7 % of hydrogen content, 0.17 % of nitrogen content, 0.33 % of ash content and 7% of moisture content. The electric field effect on the thermal decomposition of biomass pellets and combustion of volatiles was studied using a positively biased electrode axially inserted through the biomass layer, with its top located at the bottom of the combustor. The positive bias voltage of the electrode relative to the grounded walls of the combustor was varied in the range from 0.6 kV to 2.7 kV by limiting the current to 5-6 mA in the space between the electrodes.
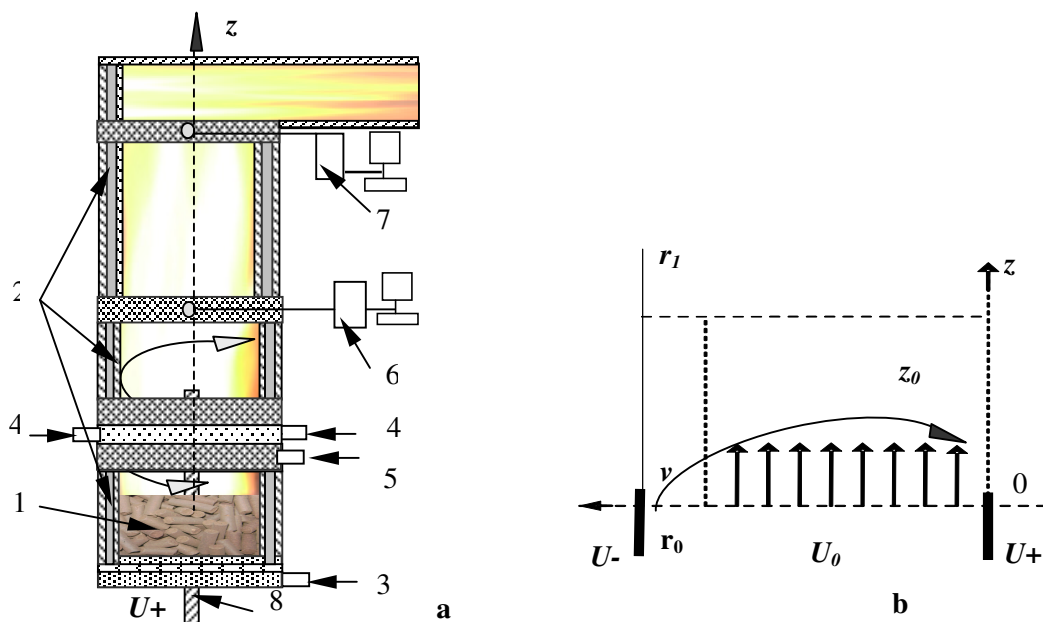
Fig. 1. **Pilot device for experimental study of the electric field effect on biomass thermo chemical conversion (a) and principal computational domain (b):** 1 – biomass gasifier; 2 – water-cooled sections of the combustor; 3 – primary axial air supply; 4 – secondary swirling air supply; 5 – propane flame supply; 6, 7 – orifices for diagnostic tools; 8 – positively biased electrode

The experimental study of the electric field effects on the flame characteristics includes joint measurements of the flame velocity, temperature composition fields and using the methodology described in [6]. The electric field effect on the heat output and produced heat energy is estimated from the calorimetric measurements of the cooling water flow [6].

Mathematical modelling

A 2D axially-symmetric, compressible, swirling flow (density ρ, velocities u_r, u_z, u_φ) in a cylindrical pipe (Fig.1-b) with the radius $r_0 = 0.05$ m and length $z = z_0 = 0.1$ m, with simple chemical reaction (mass-fraction of the reactant C, temperature T) is described by four Eyler and two reaction-diffusion dimensionless equations in the cylindrical coordinates (r, z) at a time t. The equations were made dimensionless by scaling the lengths to r_0, the pressure p to $p_0 = \rho_0 U_0^2$ N·m^{-2} and the meridian components of the current density vectors (j_r, j_z)

$$j_r = -\frac{1}{\mu}\frac{\partial B_\phi}{\partial z}, \, j_z = \frac{1}{\mu r}\frac{\partial (rB_\phi)}{\partial r} \text{ to } j_0 = \frac{I}{2\pi r_0^2} = 63.66 I \text{ A·m}^{-2}.$$

The azimuthal component of the induced magnetic field B_φ was scaled to

$$B_0 = \frac{\mu I}{2\pi r_0^2} = 0.4 \cdot 10^{-5} \cdot I \text{ N} \cdot (\text{A} \cdot \text{m})^{-1},$$

the electromagnetic forces

$$F_r = -B_\varphi j_z, \ F_z = B_\varphi j_r \text{ to } F_0 = j_0 \cdot B_0 = 0.25 \cdot 10^{-3} \cdot I^2 \text{ N} \cdot \text{m}^{-3},$$

the special heat release

$$B^* \text{ to } B^*_0 = c_p \cdot T_0 = 1.5 \cdot 10^6 \text{ J} \cdot \text{kg}^{-1},$$

the reaction-rate pre-exponential factor

$$A \text{ to } A_0 = \frac{U_0}{r_0} = 10^4 \ 1 \cdot \text{s}^{-1},$$

the activation energy

$$E \text{ to } E_0 = R \cdot T_0 = 2.5 \cdot 10^4 \text{ J} \cdot \text{mol}^{-1},$$

and at the inlet the density to $\rho_0 = 1 \text{ kg} \cdot \text{m}^{-3}$, the velocities to $U_0 = 0.01 \text{ m} \cdot \text{s}^{-1}$, the circulation $v = u_\varphi \cdot r$ to $V_0 \cdot r_0$, the temperature to $T_0 = 300$ K, the mass-fraction to $C_0 = 1$, where $R = 8.314 \text{ J} \cdot (\text{mol} \cdot \text{K})^{-1}$ is the universal gas constant, $c_p = 1000 \text{ J} \cdot (\text{kg} \cdot \text{K})^{-1}$ is the specific heat at a constant pressure, $\mu = 4\pi \cdot 10^{-7} \text{ N} \cdot \text{A}^{-2}$ is the magnetic permeability in the medium, the electric current I changes from 0 to 0.63 A with the time step 0.063.

For the dimensionless parameters r, $x = z/r_0$, $(x_0 = z_0/r_0)$, ρ, $u = u_r/U_0$, $w = u_z/U_0$, v, T, C the electric field effect on the flame characteristics can be estimated from the following equations:

$$
\begin{cases}
\dfrac{\partial \rho}{\partial t} + \dfrac{1}{r}\dfrac{\partial (r\,u\rho)}{\partial r} + \dfrac{\partial (w\rho)}{\partial x} = 0, \\[2mm]
\dfrac{\partial (\rho\,u)}{\partial t} + \dfrac{1}{r}\dfrac{\partial (r\,u\rho\,u)}{\partial r} + \dfrac{\partial (w\rho\,u)}{\partial x} = S^2\rho\dfrac{v^2}{r^3} - \dfrac{\partial p}{\partial r} + P_e F_r, \\[2mm]
\dfrac{\partial (\rho\,w)}{\partial t} + \dfrac{1}{r}\dfrac{\partial (r\,u\rho\,w)}{\partial r} + \dfrac{\partial (w\rho\,w)}{\partial x} = -\dfrac{\partial p}{\partial x} + P_e Fx, \\[2mm]
\dfrac{\partial (\rho\,v)}{\partial t} + \dfrac{1}{r}\dfrac{\partial (r\,u\rho\,v)}{\partial r} + \dfrac{\partial (w\rho\,v)}{\partial x} = 0, \\[2mm]
\dfrac{\partial (\rho\,T)}{\partial t} + \dfrac{1}{r}\dfrac{\partial (r\,u\rho\,T)}{\partial r} + \dfrac{\partial (w\rho\,T)}{\partial x} = \dfrac{L_e}{P_e}\Delta T + \beta A\rho C \exp\left(-\dfrac{\delta}{T}\right), \\[2mm]
\dfrac{\partial (\rho\,C)}{\partial t} + \dfrac{1}{r}\dfrac{\partial (r\,u\rho\,C)}{\partial r} + \dfrac{\partial (w\rho C)}{\partial x} = \dfrac{1}{P_e}\Delta C - \rho AC \exp\left(-\dfrac{\delta}{T}\right),
\end{cases}
\tag{1}
$$

where $\Delta q = \dfrac{1}{r}\dfrac{\partial}{\partial r}(r\dfrac{\partial q}{\partial r}) + \dfrac{\partial^2 q}{\partial x^2}$ is the Laplace operator $(q = T; C)$;

$P_e = \rho_0 \cdot U_0 \cdot r_0/D = 10$ and $L_e = \lambda/(c_p \cdot D) = 1$ – are the Peclet and the Lewis numbers;

$S = V_0/U_0 = 1; 3; 5$ is the swirl number;

$P_e = F_0 \cdot r_0/(\rho_0 \cdot U_0^2)$ is the electrodinamic force parameter changes from 0 to 1 with the time step 0.1;

$\beta = B^*_0/(c_p \cdot T_0) = 5$ and $\delta = E_0/(R \cdot T_0) = 10$ are the scaled heat-release and activation-energy;

$\lambda = 5 \cdot 10_{-2} \text{ J} \cdot (\text{s} \cdot \text{m} \cdot \text{K})^{-1}$ is the thermal conductivity;

$D = 5 \cdot 10^{-5} \text{ m}^2 \cdot \text{s}^{-1}$ is the molecular diffusivity;

$A = 50000$, $F_r = -\dfrac{B_\phi}{r}\dfrac{\partial (rB_\phi)}{\partial r}$, $Fx = -B_\phi\dfrac{\partial B_\phi}{\partial x}$.

From the Maxwell's equations and Ohm's law for B_φ follows the equation

$$\frac{\partial B_\phi}{\partial t} + \frac{\partial (uB_\phi)}{\partial r} + \frac{\partial (wB_\phi)}{\partial x} = 0.$$

For the dimensionless pressure p we consider a model for perfect gas $p = \rho \cdot T$, where the unknown functions are: $\rho, u, w, v, T, C, B_\varphi$ [7; 8].

The boundary conditions (BC) are the following:

1. along the axis $r = 0 - u = v = 0$, $\psi = 0$, $\partial T / \partial r = \partial C / \partial r = \partial w / \partial r = 0$, $B_\varphi = 0$;

2. at the wall $r = 1$ – $u = v = 0$, $\psi = q$, $\partial w / \partial r = \partial C / \partial r = 0$, $\partial T / \partial r + Bi(T - 1) = 0$, $B_\varphi = B_0 \cdot (1 - x/x_0)$ (uniform distribution of $j_r = const$);

3. at the pipe outlet $x = x_0 = 2$ – u = 0, $B_\varphi = 0$, $\partial T / \partial x = \partial C / \partial x = \partial w / \partial x = \partial v / \partial x = \partial \psi / \partial x = 0$;

4. at the pipe inlet $x = 0$ – $u = 0$, $T = 1$, for $r \in [0,1]$ and $w = 1$, $C = 1$, $\psi = 0.5\,r^2$, $v = 0$, for

   $r \in [0, r_1]$; $\psi = q$, $v = 4r \dfrac{(r - r_1)(1 - r)}{(1 - r_1)^2}$, $w = 0$, $C = 0$ we have a uniform jet flow at $r < r_1$ and

   rotation at $r > r_1$ with the maximum azimuthal velocity 1 at $r = (1 - r_1)/2$; $B_\varphi = B_0/r$ for

   $r \in [r_*, 1]$ $(j_z = 0)$ and $B_\phi = \dfrac{B_0}{r}(1 - \sqrt{1 - \dfrac{r^2}{r_*^2}})$ for $r \in [0, r_*]$ (real nonuniform distribution of

   $j_z \neq 0$ [9] (Fig. 1-b). Here $Bi = \dfrac{hr_0}{\lambda} = 0.1$ is the Biot number, $q = \dfrac{r_1^2}{2} = 0.125$ is the

   dimensionless fluid volume, $r_1 = 0.5$, $r_* = 0.2$, h = 0.1 J·(s m^2·K)$^{-1}$.

The linear stability of the flow with simple chemical reaction was investigated in [10]. To solve a discrete problem with 40 x 80 uniform grid points and the time step 0.0008, the ADI method of Douglas and Rachford [11] was used. The maximum value of the reaction rate $R^* = A \cdot C \cdot exp\,(\delta/T)$ was obtained with the maximum error 10^{-7} for the iterative process. The perfect gas model was used because of faster convergence.

Results and discussion

The results of the numerical simulation of the axial distribution of the main undisturbed ($P_e = 0$) flame characteristics (T, u_z, u_r) and the formation of the flow stream function at a high swirl level close to the swirling flow inlet ($S = 3$) are illustrated in Figures 2, a-d.
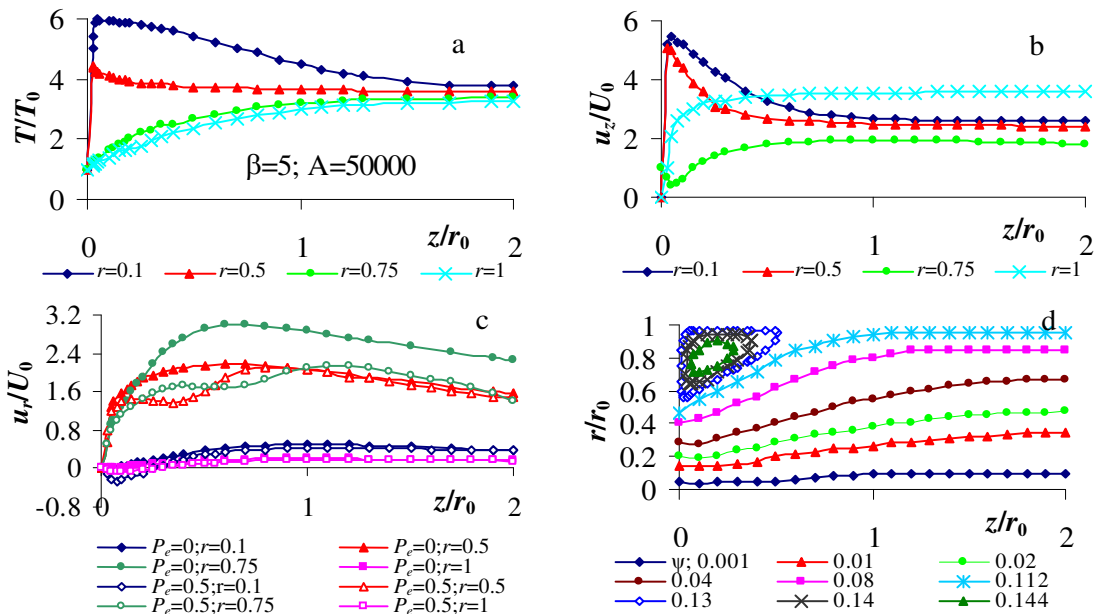
Fig. 2. **Axial distribution of the flame temperature (a), axial (b) and radial (c) flame velocity components and spatial distribution of the stream function (d)**

With the high swirl intensity $S = 3$ and swirl-enhanced mixing of the flame components, the peak values of the dimensionless flame temperature and axial velocity (u_z/U_0) are detected in the central part of the swirling flame flow ($r < 0.5$) with a fast decrease downstream the flame axis (Figures 2-

a, b). An increase of the flame temperature and axial flow velocity is observed along the outside part of the flame ($r > 0.5$) indicating the radial expansion of the flame reaction zone in the flame downstream regions. The axial distribution of the radial component (u_r) downstream the flame axis ($r < 0.5$) (Fig. 2-c) is influenced by the formation of local vortices at the flow inlet, close to the channel walls (Fig. 2-d) and determining an uneven increase of the radial flow velocity up to the peak value at the primary stage of the flow field formation ($z/r_0 < 1$). Moreover, the local formation of the inlet flow vortices at $z/r_0 < 0.5$ is responsible for the radial flow reversing that is detected close to the channel walls ($r > 0.5$). The stabilization of the flow stream function along with the stabilization of the axial distribution of the radial flow velocity is observed further downstream ($z/r_0 > 1$), where the decrease of the flame temperature results in the correlating decrease of the radial flow velocity.

Table 1

Maximum values of the reaction rate (Max *R*), axial velocity (Max *w*), radial velocity (Max *u*), stream function (Max *Ψ*), temperature (Max *T*), minimum density (Min *ρ*) and averaged temperature (Aver *T*) versus the inlet flow swirl number

S	P_e	Max R	Min ρ	Max w	Max u	Max Ψ	Max T	Aver T
1	0	299.77	0.018	6.18	2.63	0.1428	5.9724	3.891
3	0	299.80	0.015	6.19	3.09	0.1395	5.9727	3.973
5	0	299.87	0.014	6.20	3.48	0.1374	5.9730	4.024

The decreasing swirl intensity and mixing rate of the reactants show the influence on the development of the flame reaction zone determining a gradual decrease of the reaction rate, peak and average values of the flame temperature, axial and radial velocity components (Table 1) by increasing the length of the flame reaction zone. This is confirmed by the experimental measurements of the axial distribution of the average values of the swirling flame temperature and axial velocity within the limit of the low swirl number at the combustor inlet ($S \approx 0.3$) when gradual mixing of the axial flow of volatiles (CO, H_2) results in the increase of the length of the flame reaction zone up to $z/r_0 = 10$ (Fig. 3).
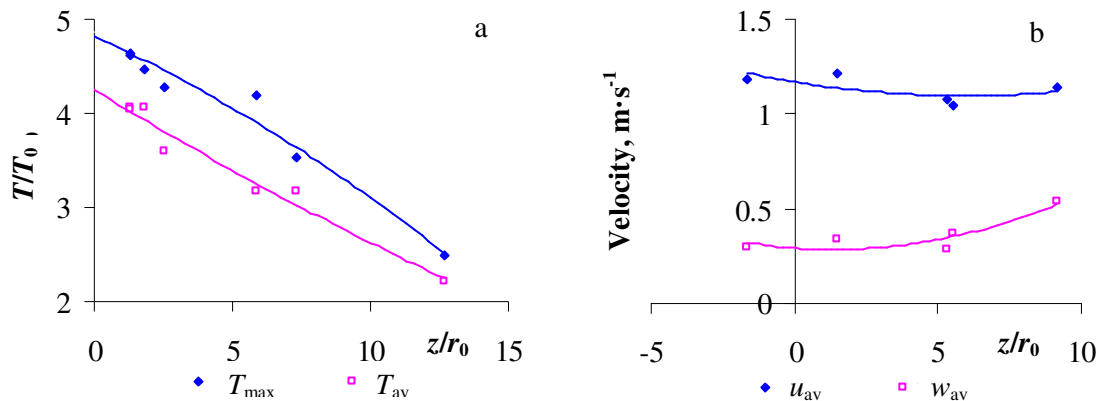
Fig. 3. **Axial distribution of the peak and average values of the flame temperature (a); axial and tangential flow velocities (b) at low swirl number (*S* = 0.3) at the combustor inlet**

If the radial electric field is applied to the flame base, the field-induced variations of the main flame characteristics are observed. Numerical estimation of the electric current distribution between the electrodes for the given field configuration has revaled the peak current levels at the flow inlet ($z/r_0 = 0.1$) with a fast decrease further downstream (Fig. 4-a). Hence, the dominant field effect on the flame characteristics can be related to the primary stage of swirling flow formation, when the field-induced increase of the maximum value of the stream function at a high swirl number of the inlet flow ($S = 3$) results in field-enhanced formation of the local vortices (Fig. 4-b) along with the field-enhanced mixing of the flame components and correlating increase of the maximum value of the reaction rate (Fig. 4-c) that decreases the average values of the flame temperature (Fig. 4-d), the radial flow velocity at the primary stage of the flow formation (Fig. 2-c) and the maximum value of the

radial velocity (Fig. 4-e) at a nearly constant maximum value of the peak flame temperature. Moreover, the field-induced formation of the local flow of vortices at the primary stage of the flame flow formation results in a field-induced decrease of the maximum value of the axial velocity at $P_e < 0.4$, whereas the field-enhanced increase of the reaction rate promotes the correlating increase of the maximum value of the axial flow velocity at $P_e > 0.4$ (Fig. 4-f).
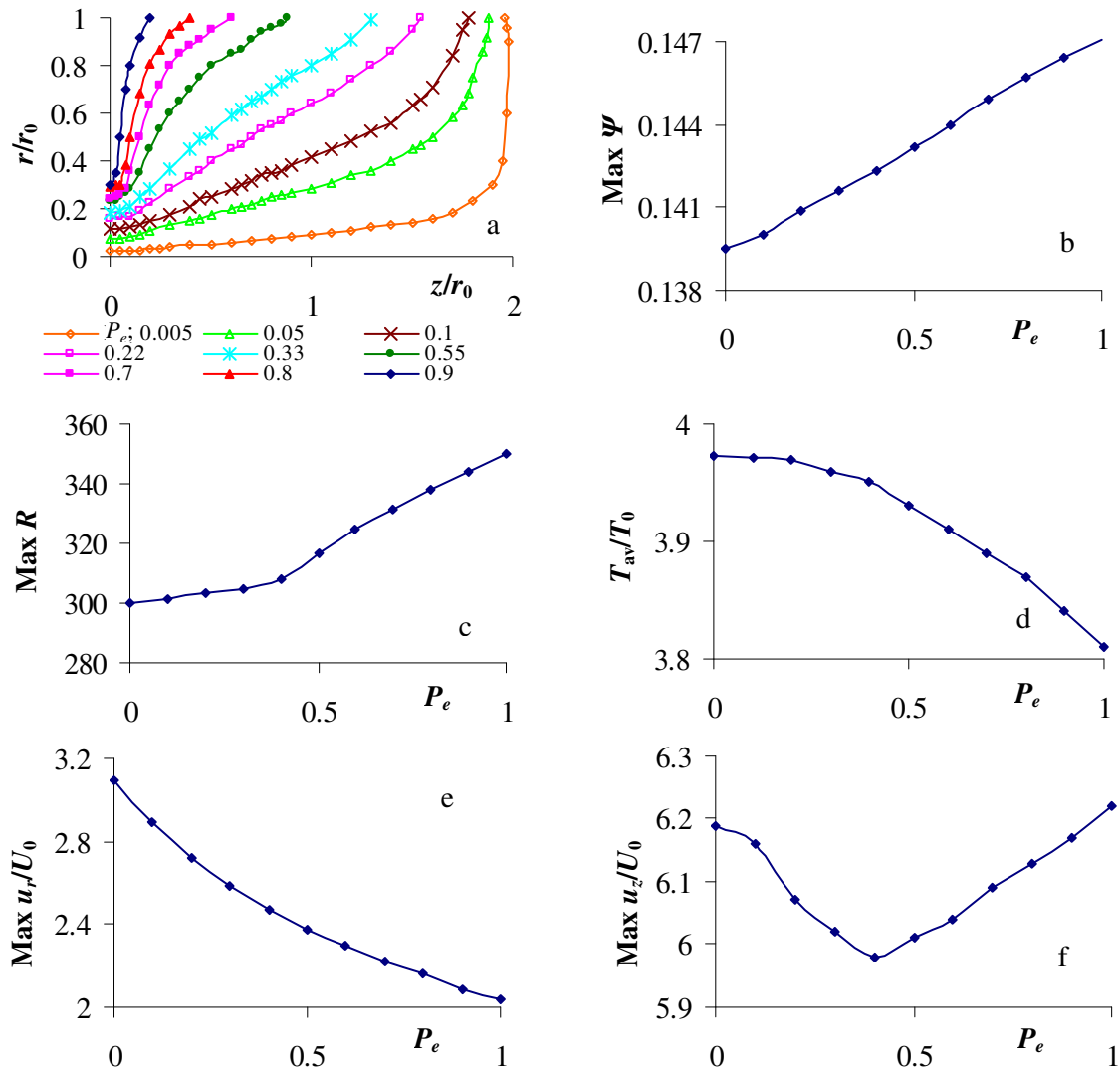
Fig. 4. **Spatial distribution of the electric current between the electrodes (a) and the electric field induced variation of the maximum values of a stream function and the reaction rates (b, c), average value of the temperature (d) and maximum values of the radial and axial flow velocity components (e, f).**

The experimental study of the electric field effect at a low swirl number of the inlet flow at the bottom of the combustor ($S = 0.3$) has shown similar field-induced variations of the average value of the flame temperature, axial and tangential flow velocity components (Figures 5-a, b). By analogy with the processes developing downstream the flame reaction zone at the high swirl intensity ($S = 3$), the field-induced variations of the combustion characteristics at the low swirl intensity ($S = 0.3$) can be attributed to the competitive processes of the field-enhanced mixing of the flame components at the primary stage of the flame formation, improving thus the field-enhanced combustion conditions with the increased rate of thermo chemical conversion of biomass pellets and completing the combustion of the volatiles (CO, H_2). The improvement of the combustion conditions results in field-enhanced increase by about 7-10 % of the volume fraction of CO_2 in the products (Fig. 5-c) and the produced heat energy at thermo chemical conversion of biomass pellets (Fig. 5-d).
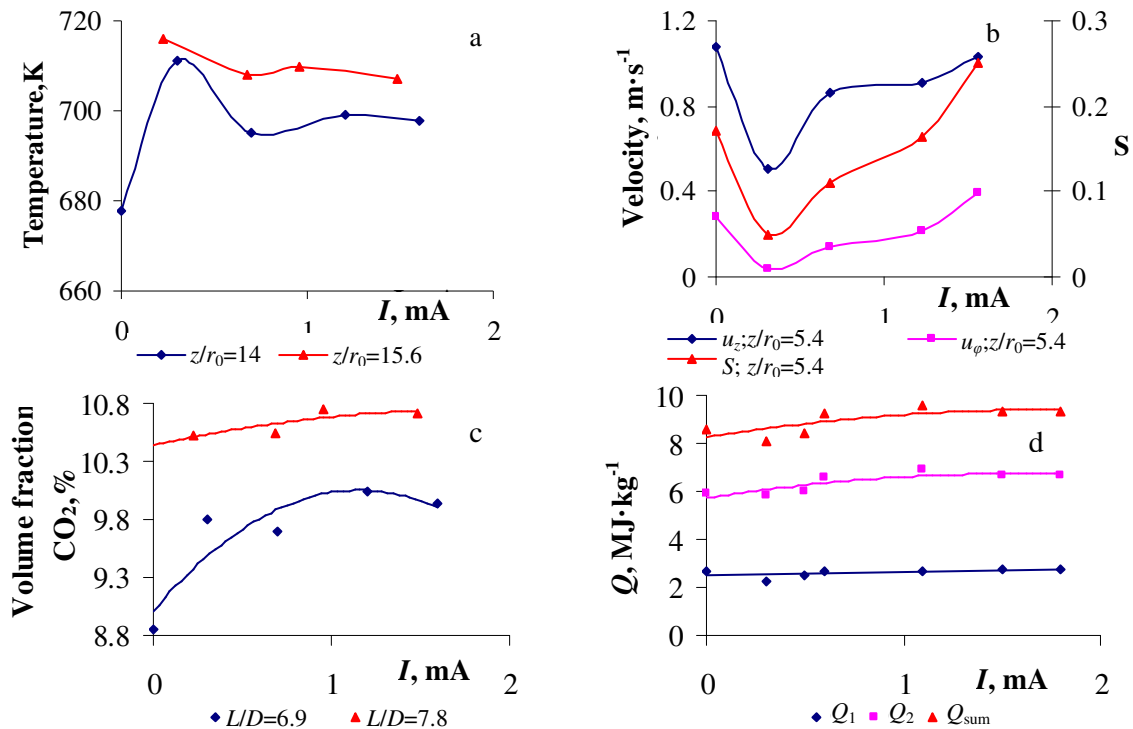
Fig. 5. **Electric field induced variations of the peak and average values of the flame temperature (a), axial and tangential values of the flow velocity and flow swirl number (b), composition of the products (c) and the produced heat energy in the combustor (d)**

Conclusions

1. The results of the mathematical modelling and numerical simulation allow to conclude that with the high swirl intensity ($S = 3$) the swirl-enhanced mixing of the flame components results in formation of an axial reaction zone with fast decrease of the peak flame temperature and velocity and with radial expansion of the reaction zone in the flame downstream regions.

2. The experimental results show that with the low swirl intensity ($S = 0.3$) the development of the reaction zone is limited by gradual mixing of the reactants with the resulting increase of the reaction zone length.

3. The results of the numerical simulation evidence that formation of the flame reaction zone is influenced by the electric field-induced variations of the flow stream function promoting the field-enhanced formation of the local vortices and mixing of the reactants by increasing the reaction rate.

4. By analogy with the processes developing at the high swirl intensity ($S = 3$), the field-induced variations of the main flame characteristics at the low swirl intensity (0.3) confirm the electric field-enhanced mixing of the reactants resulting in more complete combustion of the volatiles downstream the flame reaction zone with correlating increase of the produced heat energy.

Acknowledgments

Referencess

1. Gupta A.K., Lilley D.G., Syred N. Swirl Flows. Abacus Press UK, 1984, 588 p.
2. Nussbaumer T. Combustion and Co-combustion of Biomass: Fundamentals, Technologies, and Primary Measures for Emission Reduction. Energy&Fuels, 2003, vol.17, pp. 1510-1521.

3. Colannino J. Electrodynamic Combustion Control^{TM} Technology. A Clear Sign White Paper, ClearSign Combustion Corporation, Seattle, 2012, [online][15.01.2016] Available at: http://www.clearsign.com/wp-content/uploads/2012/07/ClearSign-Whitepaper-2012-06-18.pdf.
4. Sumathi Swaminathan. Effects of magnetic field on micro flames. A Thesis of master of Science in Mechanical Engineering in The Department of Mechanical Engineering, 2005, p. 125. [online][15.01.2016] Available at: http://etd.lsu.edu/docs/available/etd-11182005-092209/unrestricted/Swaminathan_thesis.pdf.
5. Zake M., Barmina I., Turlajs D., Lubane, M., Krumina A. Swirling Flame, Part 2. Electric field effect on the soot formation and greenhouse emissions. Magnetohydrodynamics, vol. 40, Issue 2, 2005, pp. 183-202.
6. Barmina I., Purmalis M., Valdmanis R., Zake M. Electrodynamic control of the combustion characteristics and heat energy production, Combustion science and technology, vol. 188, Issue 2, 2016, pp. 190-206, [online][15.01.2016] Available at: http://www.tandfonline.com/doi/abs/10.1080/00102202.2015.1088010.
7. Choi J.J., Rusak Z., Kapila A.K. Numerical simulation of premixed chemical reactions with swirl. Combustion theory and modelling, vol. 6(11), 2007, pp. 863-887.
8. Kalis H., Marinaki M., Strautins U., Lietuvietis O. On the numerical simulation of the combustion process with simple chemical reaction. Proc. of the 7-th Baltic Heat Transfer conf. "Advances in Heat Transfer, aug. 24-26, 2015, pp. 175-180.
9. Boyarevitch V.V., Freiberg Y.Zh., Shilova E.I., Therbinyn E.V. Electro- vortexed flows, Zinatne Press, Riga, in Russian, 1985, 315 p.
10. Koliskina V., Kolyshkin A., Volodko I., Kalis H. On the stability of convective motion generated by a chemically reacting fluid in a pipe, Proc. of the 13 Intern. Conf. "On numerical analysis and applied mathematics", 2015, pp. 11-14.
11. Douglas J., Rachford R. On the numerical solution of heat conduction problems in two and three space variables, Trans. Amer. Math.Soc., vol. 82(2), 1956, pp. 421-439.